International Journal of Natural and Engineering Sciences
E-ISSN: 2146-0086 18(1): 55-76, 2024
Research Article

The volatile composition of Turkish propolis with SPME-GCMS and it's *in silico* anti-inflammatory effects

Nilüfer Vural[1,2] *, Sibel Kaymak[1]

[1]*Department of Traditional, Complementary and Integrative Medicine, Biotherapeutic Products Research and Development Program, Institute of Public Health, Ankara Yıldırım Beyazit University, 06010 Etlik/Ankara/Türkiye*
[2]*Department of Food Processing, Vocational School of Health Services, Ankara Yıldırım Beyazit University, 06760 Çubuk/Ankara/Türkiye*

* Corresponding author: nilufervural@aybu.edu.tr

(Received: February 14, 2024 / Accepted: March 12, 2024)

Abstract

Propolis, colloquially termed 'bee glue,' is a naturally occurring substance synthesized by bees, acclaimed for its therapeutic attributes and anti-inflammatory effects. The primary objective of this investigation is to explore the anti-inflammatory properties of the volatile compounds present in propolis. In this study, in silico drug discovery methodologies are employed to identify these compounds and ascertain their pharmacological targets. The research commences with the identification of volatile compounds within propolis and the prediction of their pharmacological targets using network pharmacology. Subsequently, molecular docking analyses are conducted to assess the binding affinity of these volatile compounds with key inflammatory proteins. This methodology yields insights into the potential of propolis's volatile bioactive compounds to selectively inhibit the activity of crucial inflammatory targets, including NLRP3 and cyclooxygenase-2 (COX-2). The findings of this investigation reveal that the volatile compounds within propolis demonstrate the potential to selectively inhibit the activity of significant inflammatory targets, particularly NLRP3 and COX-2. Volatile constituents of propolis may hold promise for therapeutic interventions in various inflammatory diseases, with a specific emphasis on respiratory diseases.

Keywords: Propolis; Volatile compounds; Molecular docking; Inflammation.

Introduction

Apitherapy constitutes a form of complementary medicine utilizing bee products for therapeutic purposes. These products include honey, propolis, royal jelly, bee venom, and their derivatives [1]. The application of bee products has emerged as an alternative treatment modality spanning oncological [2] to chronic conditions such as cardiovascular issues [3], diabetes [4], and rheumatic diseases [5]. Propolis, among the spectrum of bee products, ranks prominently as a beehive compound following honey [6]. Originating as a resinous substance with robust adhesive properties, bees manufacture propolis from diverse floral secretions to seal hive apertures and fortify hive entrances against intruders [7]. Propolis boasts diverse biological and pharmacological attributes, including antibacterial [8], antifungal and immunomodulatory [9], antiviral [10], cholesterol modulation [11], and anti-inflammatory [12] properties.

Literature attests to the potent anti-inflammatory efficacy of propolis across various diseases [13-14]. Studies on Japanese propolis investigated inhibitory effects on in vitro basophil activation to elucidate its impact on allergic inflammation [15]. Concurrently, Chilean propolis has been studied for in vivo anti-inflammatory potential against 12-O-tetradecanoyl-phorbol-13-acetate and arachidonic acid inflammatory agents [16]. Another investigation, using similar biomarkers as our study, focused on the effects of Korean propolis on gastric inflammation [17]. Results indicated a significant decrease in interleukins, TNF-alpha, cyclooxygenase-2 (COX-2), and inducible nitric oxide synthase activity with propolis treatment. Inflammasomes, crucial regulators of interleukins, are intricately linked to diseases and various immunological pathways [18]. Notably, the NLRP3 inflammasome plays a pivotal role in numerous inflammatory diseases, including myocarditis and pneumonia [19]. Activation of NLRP3 inflammasomes involves the upregulation of

NLRP3 and certain interleukins. Consequently, inhibiting the NLRP3 protein is posited to mitigate NLRP3 inflammasome activity and associated inflammation [20]. A study on inflammatory bowel disease demonstrated that inhibiting NLRP3 activity with MCC950 significantly reduced disease symptoms in models [8]. Employing a similar inhibition approach in another study revealed that NLRP3 inhibition alleviated glial responses, exerting an anti-inflammatory effect, and potentially offering a novel treatment avenue for chemotherapy-induced cognitive impairment [21].

Utilizing in-silico analysis, molecular docking experiments were conducted to explore the molecular suppressor activity of select ligands against neuroinflammation proteins associated with Alzheimer's disease, specifically targeting NLRP3 [22], and multiple sclerosis [23]. Notably, Caspase-1 stands out as a pivotal stimulatory component integral to the maturation of inflammatory cytokines. Given their shared metabolic pathways, NLRP3 and caspase-1 exhibit a close interrelation, jointly activating the NLRP3 inflammasome. NLRP3 regulates the assembly of the inflammasome complex, recruiting caspase-1 to this structure. Upon caspase-1 activation, pro-inflammatory cytokines are cleaved and activated, culminating in the production of mature IL-1β and IL-18 [24]. In a noteworthy anti-inflammatory investigation involving caspase-1 inhibition, it was realized that the *Coptis chinensis* plant extract effectively inhibits caspase-1 activity, thereby diminishing inflammation levels in experimental models [25]. Furthermore, *Phyllanthus nivosus* leaf extracts demonstrated significant potential in reducing inflammation by suppressing caspase-1 activity. Cyclooxygenases, other important factors in inflammation, are responsible for producing prostaglandins during inflammatory processes. The initial release of arachidonic acid is facilitated by the catalysis of phospholipase A2 (PLA2), followed by the formation of prostaglandins through the activity of COX-1 and COX-2 [26-27]. Extensive literature underscores the anti-inflammatory properties associated with COX-2 and PLA2 inhibition across diverse diseases and experimental models [28-29].

This study investigated the anti-inflammatory properties of volatile organic compounds within propolis. Briefly, propolis samples were extracted, and volatile compounds were analyzed using solid phase microextraction (SPME) and Gas Chromatography/Mass Spectrometry (GC-MS) methods. The anti-inflammatory effects of these volatile extracts were assessed through in-silico molecular docking methodologies targeting key components in the inflammatory cascade, including NLRP3, caspase-1, COX-2, and PLA2. The inhibitory activities of each compound were scrutinized, considering both binding poses and energies. Additionally, reference inhibitor molecules underwent similar analyses to facilitate a comparative assessment of inhibitor activity across models. Results indicate that propolis constituents collectively manifest anti-inflammatory effects, employing a comparable inhibitory mechanism across diverse targets. Given the gradual reduction in the efficacy of continually consumed anti-inflammatory drugs, there exists a growing emphasis on the development of derivatives in modern synthetic organic chemistry. This work seeks to contribute to this ongoing effort by synthesizing novel derivatives of existing drugs.

Materials and Methods

Beehive Material

Propolis samples were collected from an *Apis mellifera* L. beehive at the Ankara Yildirim Beyazit University, Biotherapeutic Product Research and Development Unit at the Department of Traditional, Complementary, and Integrative Medicine in May/2022. Samples were immediately analyzed after harvesting.

Chemicals and Materials

SPME fibers of StableFlexTM coated with carboxen/polydimethylsiloxane (CAR/PDMS, 75μm), divinyl benzene/polydimethylsiloxane (DVB/PDMS, 65 μm), and polydimethylsiloxane (PDMS, 100 μm) were purchased from Supelco (Oakville, ON, Canada).

Volatile Analysis

The volatile analysis utilizing Headspace Solid-Phase Microextraction (HS-SPME) was conducted following recent protocols with slight adaptations [30]. Beehive propolis (250 mg) was placed into SPME screw cap vials (10 mL). SPME fibers, temperature-conditioned (250 °C, 10 min), were manually inserted into vials containing propolis samples and sealed using a crimper. Subsequently, the vials were placed on a heating table,

maintained at 70 °C for 40 min to allow adsorption of volatile compounds onto SPME fibers. These fibers were then withdrawn into a needle and subsequently injected into the GC–MS port.
GC–MS analysis was executed using a Shimadzu GC-2010 gas chromatogram equipped with a Flame Ionization Detector and a DB-5 column (30 m, 0.25 mm, 0.25 mm film thickness; Supelco), coupled to a Shimadzu QP2010-Plus mass spectrometer. The injector and interface temperatures were set at 250 °C, while the ion source temperature was set at 220 °C. A gradient temperature program was employed for volatiles analysis, initiating with the oven temperature held at 40 °C for 2 min, followed by an increase to 200 °C at a rate of 3 °C/min, held for 10 min. Subsequently, a ramp of 5 °C/min at 250 °C was implemented, held for 5 min, and a final ramp of 5 °C/min at 275 °C. The Split injection mode was used at a ratio of 1/50. To prepare the SPME fiber for other analyses, it was placed in the injection port for 10 min at 220 °C to ensure complete elution of volatiles. Blank runs were conducted during sample analyses. The Flame Ionization Detector was maintained at a temperature of 300 °C, and the quadrupole mass spectrometer operated in Electron Impact (EI) mode at 70 eV, with a scan range set at m/z 40–700 [31].

GC–MS Data Processing

The identification of volatile compounds in propolis involved a comparative analysis of retention times and spectra with established standards. Compounds were identified by correlating their relative retention times to a C8–C32 n-alkanes mixture and matching mass spectra with data from the NBS75K, Wiley 7, NIST7MS search 2.0 library within the GC-MS system. Additionally, comparisons were performed with literature data and standards for the principal components. The validity of the results was further confirmed through the comparison of compound elution order and relative retention indices on a DB-5 column. All analyses were conducted in triplicate to ensure the robustness and reliability of the findings.

Network Pharmacology

Network pharmacology emerges as a potent methodology for the selection of target proteins, offering the capacity to integrate diverse biological data sources and discern potential drug targets based on their strategic placement and significance within biological networks [32]. In the present study, network pharmacology was employed for target selection. The 'inflammatory response' term was input into the 'Pathway / Process / Disease' module of STRING 11.5, facilitating the specification of inflammatory targets and subsequent protein-protein interaction (PPI) analysis. Utilizing the 'Multiple Proteins' module, the analysis was conducted with the species set as 'Homo sapiens,' and a confidence level of ≥0.400 was established. The obtained results were then imported into Cytoscape 3.7.2 for data visualization and further analysis.

In Silico Molecular Dockings

The structures of NLRP3 (PDB ID: 7ALV), caspase-1 (PDB ID: 1RWK), COX-2 (PDB ID: 5KIR), and PLA2 (PDB ID: 1TD7) were retrieved from the Protein Data Bank, with each protein serving as a rigid receptor in the subsequent docking simulations. The preparation of proteins for docking involved the following steps: (i) energy minimization, employing 100 steepest descent steps with a 0.02 Å step size and an update interval of 10, (ii) removal of water molecules, (iii) deletion of solvent and non-complex ions, and (iv) addition of polar hydrogen atoms and AM1-BCC charges [33]. Ligand structures, acquired in sdf format, were retrieved from the PubChem database. The preparation of all ligands followed a procedure similar to that of protein preparation, with the addition of charges based on the Gasteiger charge model [34].
In this study, semi-flexible molecular docking simulations were conducted using AutoDock Vina. This approach allows ligand conformations to adjust, seeking the minimum protein binding energy while keeping the proteins in a stable state [35]. Initially, the blind docking method was employed to explore protein binding sites. A known inhibitor of the target protein was used as a ligand, and the entire protein area was searched to identify optimal binding positions. Subsequently, oriented docking was carried out using the resultant coordinates, focusing on the smaller area identified during blind docking, as it offers the most stable interaction conformations [36]. Molecular docking was then executed to examine inhibitory interactions between volatile organic compounds of propolis and target inflammatory proteins. Post-docking, results with score values above -5, according to the AutoDock Vina algorithm and energy range, were disregarded [37]. Finally, the top 2 poses

with the minimum binding energy for each protein were selected for visualization using Discovery Studio Visualizer. Furthermore, for each protein target, two reference inhibitors from the literature underwent the same molecular docking experiments, and the outcomes were compared. MCC950 [38] and Oridonin [39] were chosen as reference inhibitors for NLRP3; Emricasan [40] and Minocycline [41] for caspase-1; Flurbiprofen [42] and Celecoxib [43] for COX-2; and Varespladib methyl [44] and CHEMBL-149502 ligand [45] for PLA2.

Results and Discussion

Volatile Composition of Propolis

A total of 95 volatile compounds were identified using the Solid-Phase Microextraction (SPME) detection method (Table 1).

Table 1. *Identified volatile components in propolis by SPME-GCMS*

	Volatiles compounds of Propolis				Types of SPME fiber			
					PDMS	CAR-PDMS	DVB-PDMS	
	LRI (cal)	LRI (lit)	Compound	Chemical structures of compounds	%	%	%	IM
1	538	536	Acetic acid, methyl ester	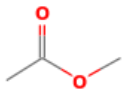	-	0,21±0,01	-	a
2	578	594	Acetic acid		-	**2,57±0,05**	**0,52±0,02**	a,b
3	654	652	2-Propanone, 1-hydroxy-	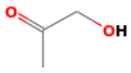	-	-	0,12±0,00	a
4	686	685	3-Buten-2-ol, 2-methyl-		-	-	0,27±0,01	a
5	720	716	3-Buten-1-ol, 3-methyl-	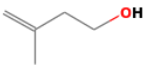	0,13±0,00	0,27±0,01	0,19±0,00	a,b
6	745	746	2-Buten-1-ol, 3-methyl-	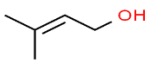	**0,51±0,03**	0,40±0,02	-	a
7	796	794	Furfural	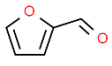	-	0,14±0,01	-	a

8	834	836	2-Methylbutanoic acid	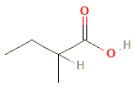	0,32±0,02	-	-	a
9	860	861	4-Pentenyl acetate		-	0,26±0,02	0,32±0,03	a,b
10	915	917	2-Buten-1-ol, 3-methyl-, acetate- Prenyl acetate	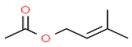	**0,86±0,06**		0,48±0,04	a
11	920	922	(+)-3-Carene	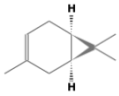	-	-	0,33±0,02	a
12	926	928	Benzaldehyde (CAS)	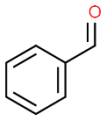	**0,53±0,03**	0,21±0,04	-	a,b
13	930	931	(-)-α-Pinene	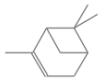	**1,12±0,03**	0,20±0,01	0,20±0,01	a,b
14	955	953	Senecioic acid	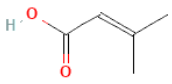	0,33±0,03	-	-	a
15	978	979	beta.-Myrcene	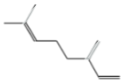	**0,53±0,05**	0,07±0,00	-	a
16	1062	1062	beta.-Terpinyl acetate	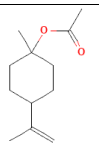	**1,19±0,12**	-	0,07±0,01	a
17	1065	1068	1,8-Cineole	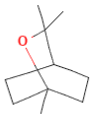	**0,45±0,08**	-	0,05±0,00	a,b
18	1067	1069	Cycloprop[a]indene, 1,1a,6,6a-tetrahydro	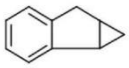	-	**2,17±0,13**	-	a
19	1076	1078	.alpha-Terpinolene	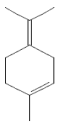	**7,19±0,56**	-	-	a,b
20	1080	1081	n-Nonanal	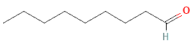	0,32±0,11	**0,63±0,03**	0,09±0,00	a

21	1081	1082	Phenylethyl Alcohol	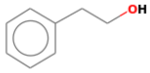	**0,71±0,12**	**0,43±0,09**	**0,58±0,09**	a,b
22	1162	1160	Benzoic acid	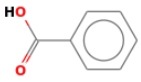	-	**1,97±0,43**	**0,95±0,32**	a,b
23	1185	1187	Benzofuran, 2,3-dihydro-	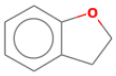	-	**6,24±0,54**	**2,88±0,12**	**a**
24	1226	1228	Phenethyl acetate	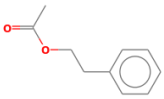	-	0,38±0,12	**0,88±0,23**	**a**
25	1228	1229	Benzene, [(2,2-dimethylcyclopropyl) methyl]-	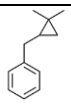	-	0,17±0,01	0,11±0,01	**a**
26	1231	1230	Benzylacetone	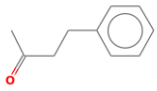	-	0,15±0,01	0,23±0,01	**a**
27	1234	1235	Cinnamaldehyde, (E)-	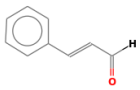	**1,23±0,02**	0,17±0,00	**1,43±0,03**	a,b
28	1236	1236	5-Hydroxymethylfurfural	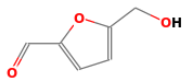	-	0,11±0,00	0,32±0,02	a
29	1266	1265	(Z)-Cinnamyl alcohol	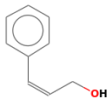	**0,97±0,09**	**1,35±0,23**	**1,54±0,19**	a
30	1296	1295	p-Vinylguaiacol	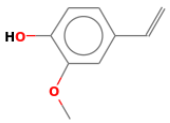	-	**0,78±0,02**	0,26±0,03	a
31	1315	1317	Benzaldehyde, 2-hydroxy-6-methyl-	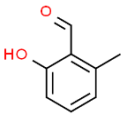	-	**3,00±0,10**	-	**a**
32	1321	1320	Benzylmalonic acid	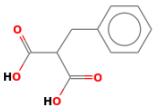	-	0,38±0,03	**0,77±0,04**	a
33	1323	1323	Benzylideneacetone	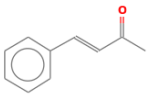	-	0,34±0,04	0,24±0,01	a
34	1324	1324	Benzaldehyde, 4-hydroxy-	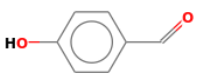	-	0,19±0,02	-	a
35	1366	1367	3,4-Dimethoxystyrene	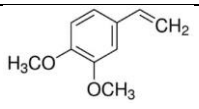	-	0,15±0,01	0,23±0,02	a

36	1383	1384	n-Decanoic acid		-	0,25±0,02	**0,97±0,05**	a,b
37	1404	1405	Farnesol	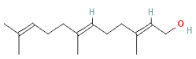	**1,56±0,09**	0,11±0,03	**1,52±0,08**	a,b
38	1406	1407	(-)-alpha-cedrene	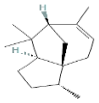	-	-	0,21±0,04	a
39	1419	1420	trans-Caryophyllene	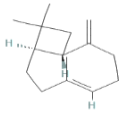	0,34±0,02	-	0,29±0,01	a,b
40	1435	1434	trans-α-Bergamotene	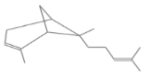	-	**0,63±0,04**	**0,70±0,05**	a
41	1436	1435	trans-Cinnamic acid	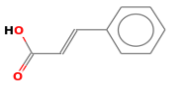	-	**0,69±0,04**	-	**a**
42	1438	1440	Cinnamyl acetate	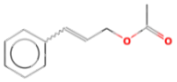	**2,14±0,12**	**2,27±0,16**	**2,46±0,18**	a
43	1454	1456	alpha.-Humulene	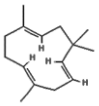	0,13±0,02	-	0,21±0,05	a
44	1465	1466	2,5-di-tert-Butyl-1,4-benzoquinone	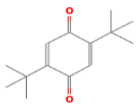	**0,84±0,14**	0,34±0,02	**1,55±0,23**	a
45	1475	1477	.beta.-Selinene	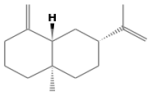	**0,54±0,02**	0,07±0,00	-	a
46	1482	1483	ar-Curcumene	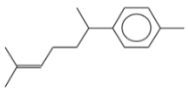	0,20±0,01	**0,53±0,04**	**1,40±0,10**	**a**
47	1486	1488	4-Pentenoic acid, 5-phenyl-	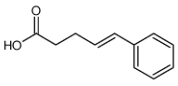	**0,97±0,09**	**8,08±0,26**	**5,09±0,12**	a
48	1491	1493	Zingiberene	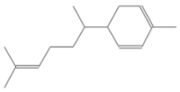	**0,69±0,04**	0,44±0,03	**1,09±0,05**	**a**
49	1496	1497	β- Bisabolene	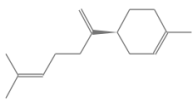	0,43±0,11	0,22±0,02	**0,72±0,08**	a,b

50	1498	1498	gamma-Muurolene	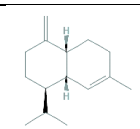	0,38±0,11	-	**0,61±0,23**	**a**
51	1508	1509	trans-α- Copaene	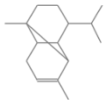	**0,51±0,18**	0,21±0,05	0,24±0,04	a
52	1515	1517	.beta.-Sesquiphellandrene	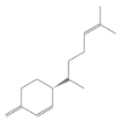	**0,77±0,05**	0,48±0,02	-	a
53	1534	1535	.alpha.-Copaen-11-ol	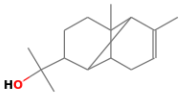	**0,58±0,03**	0,33±0,01	**1,54±0,06**	**a**
54	1536	1537	10-epi-Elemol	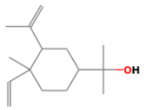	**0,76±0,02**	0,29±0,01	-	**a**
55	1562	1564	5-Phenylpenta-2,4-diecoic acid	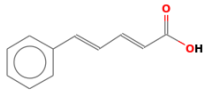	-	**3,19±0,12**	**1,64±0,13**	**a**
56	1570	1572	(-)-Caryophyllene oxide	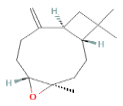	**0,59±0,02**	0,11±0,00	0,11±0,00	**a**
57	1574	1575	(+) spathulenol	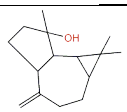	**0,76±0,04**		0,13±0,00	**a**
58	1580	1582	(+)-Cedrol	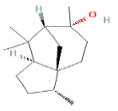	0,23±0,02	-	**0,85±0,04**	**a**
59	1596	1598	- (-)Epicedrol	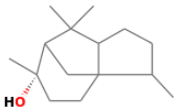		0,24±0,01	**0,85±0,06**	**a**
60	1610	1612	Hexadecane		-	**1,87±0,10**	-	**a,b**
61	1618	1619	10-epi-γ-Eudesmol	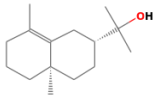	-	**1,39±0,08**	**3,73±0,12**	**a**
62	1620	1620	Thujyl alcohol	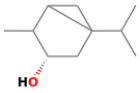	**0,54±0,03**	0,13±0,00	0,43±0,02	**a,b**
63	1634	1635	4-Hydroxycinnamic acid	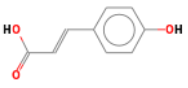	0,45±0,02	0,11±0,00	**0,54±0,03**	**a**
64	1640	1642	Δ-Cadinol	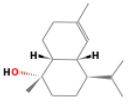	**0,58±0,06**	0,11±0,00	**1,22±0,09**	**a**

65	1644	1645	β-Eudesmol	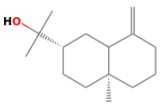	**2,8±0,07**	**2,43±0,08**	**6,54±0,11**	**a**
66	1648	1649	7-epi-β-Eudesmol	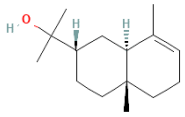	**2,60±0,06**	**2,63±0,05**	**8,55±0,19**	a
67	1655	1654	Tumerone	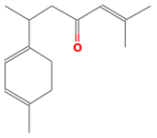	**0,57±0,05**	**0,52±0,04**	**2,16±0,09**	a
68	1656	1658	(-)-α-Bisabolol oxide	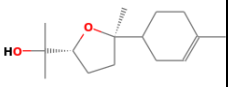	**1,74±0,11**	**1,53±0,09**	**0,12±0,02**	**a,b**
69	1662	1664	Ar-tumerone	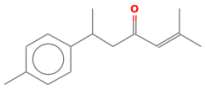	**2,12±0,09**	**2,73±0,11**	**6,16±0,17**	a
70	1664	1665	alpha-Humulene	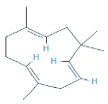	0,18±0,00	**0,54±0,06**	0,15±0,00	a
71	1666	1666	2-Propenoic acid, 3-(4-methoxyphenyl)-	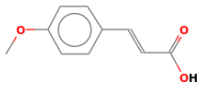	0,38±0,03	**3,78±0,23**	-	**a**
72	1680	1681	β-Turmerone	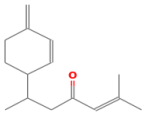		**0,79±0,06**	**1,79±0,07**	a
73	1684	1684	n-Hexyl salicylate	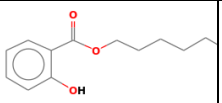		0,14±0,00	-	**a**
74	1700	1700	Heptadecane		-	0,13±0,00	-	**a,b**
75	1706	1706	(+)-epi-Bicyclosesquiphellandrene	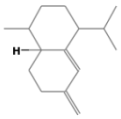		0,11±0,01	-	a
76	1740	1743	(+)-.alpha.-Atlantone	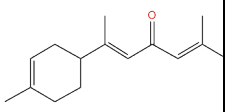		0,15±0,01	-	a
77	1747	1749	.beta.-Selinenol	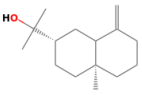		**0,97±0,04**	0,25±0,02	a
78	1766	1768	Methyl 4-methoxycinnamate	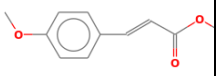	0,31±0,02	**1,09±0,05**	-	a
79	1874	1873	2-Propenoic acid, 3-(3,4-dimethoxyphenyl)-, methyl ester	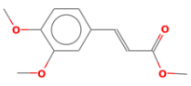		0,23±0,02	-	a

80	1875	1874	Ferulic acid methyl ester	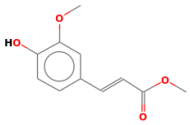	0,38±0,02	0,22±0,01		a
81	1884	1883	2-Heptadecanone		**0,66±0,04**	0,12±0,00	0,16±0,00	**a**
82	1905	1904	Hexadecanoic acid, methyl ester (CAS) Methyl palmitate		**1,26±0,08**	**0,97±0,05**	-	**a,b**
83	1960	1960	n-Hexadecanoic acid		**0,94±0,04**	**3,98±0,12**	0,11±0,00	**a,b**
84	1976	1976	Ethyl n-hexadecenoate		0,18±0,01	0,33±0,02	-	a
85	2020	2021	α-Bisabolol	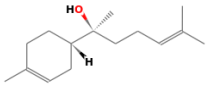	**15,18±0,78**	**15,27**±0,89	**30,9±1,13**	**a,b**
86	2052	2054	β-Nerolidol	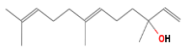	0,23±0,03	0,31±0,04	-	a
87	2065	2067	Ethanone, 1-cyclododecyl-	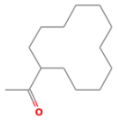		**0,79±0,03**	0,16±0,01	a
88	2085	2087	2-Nonadecanone		**2,37±0,10**	**2,64±0,09**	-	a
89	2123	2123	9-Octadecenoic acid (Z)- (CAS) Oleic acid		**0,55±0,05**	**3,48±0,12**	-	**a,b**
90	2132	2134	9,12-Octadecadienoic acid (Z,Z)-	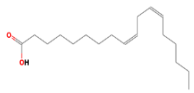	**1,28±0,08**	0,28±0,01	-	**a,b**
91	2300	2300	n-Tricosane		**3,76±0,15**	**1,98±0,09**	**1,01±0,05**	**a,b**
92	2315	2317	1,2-Benzenedicarboxylic acid, butyl octyl ester	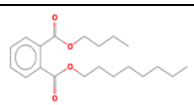	**0,51±0,04**	0,16±0,01	-	a
93	2400	2401	Pinostrobin chalcone	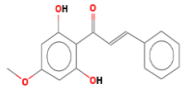	**2,39±0,11**	**0,59±0,02**	**1,13±0,04**	a
94	2403	2405	9,12-Octadecadienoic acid, methyl ester, (E,E)-		**0,58±0,02**	0,49±0,01	-	**a,b**
95	2461	2463	2-methyltetracosane	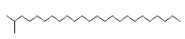	**4,28±0,21**	-	**0,78**±0,03	a

[a] Compounds listed in order of elution from a DB-5 column. b Identification of components based on standard compounds; All values are mean ± standard deviation of triplicates; LRI (cal): Linear retention indices (DB-5 column) calculated against n-alkanes. % calculated from FID data with standard LRI (lit): https://pubchem. ncbi.nlm.nih.gov; IM: Identification Method

In comparison to other studies on propolis volatiles in the literature, our results are notably extensive [46]. Across different SPME fiber types, 59 compounds were identified for PDMS, 80 for CAR/PDMS, and 63 for DVB/PDMS. The abundant compound percentages for each fiber type are presented as follows:

- PDMS Fiber: The highest to lowest compound percentages were alpha bisabolol (15.18±0.78), alpha terpinolene (7.19 ± 0.56), 2-methytetracosane (4.28±0.21), and beta-eudesmol (2.8±0.07).
- CAR/PDMS Fiber: The highest to lowest compound percentages were alpha bisabolol (15.27±0.89), 4 penteoic acid, 5-phenyl (8.08±0.26), benzofurane 2,3 dihydro- (6.24±0.54), and n-Hexadecanoic acid (3.98±0.12).
- DVB/PDMS Fiber: The highest to lowest compound percentages were alpha bisabolol (30.9±1.13), 7-epi-beta-eudesmol (8.55±0.19), beta-eudesmol (6.54±0.11), and ar-tumerone (6.16±0.17) (**Table 1**).

Target Selection and PPI Analysis

Network pharmacology analysis is a valuable tool for identifying potential drug targets across diverse diseases. In the context of this research, network pharmacology analysis was conducted to identify potential drug targets for NLRP3 inflammasome activation, a process implicated in various inflammatory diseases and serving as the initial step in the inflammatory cascade [47]. Through this analysis, we identified four potential drug targets for anti-inflammatory intervention: NLRP3 itself, caspase-1, COX-2, and PLA2. The selection of these targets was grounded in their strategic position and significance within the network of interactions between genes and proteins implicated in NLRP3 inflammasome activation (**Fig. 1**).

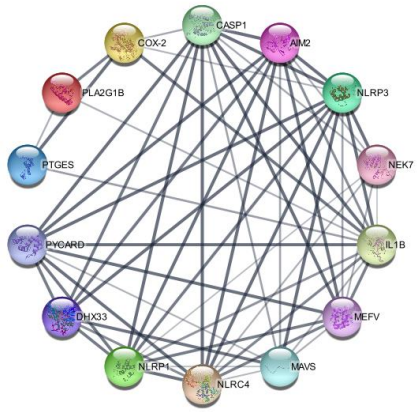

Figure 1. *Network analysis results of inflammatory proteins*

Molecular Docking

The *in silico* drug discovery experiments employed in our study have successfully identified potential inhibitors of the inflammatory response, shedding light on the physicochemical basis of inhibitory mechanisms through molecular docking. The selection of the lowest binding affinity in the docking results as a favorable docking score, with visualization of the top 2 scores, contributed to our analysis. Overall, the mean binding affinities for each protein indicate the order NLRP3 > PLA2 > COX-2 > Caspase-1, ranked from highest to lowest. The highest scores for each protein were as follows:

- NLRP3: -8.7 kcal/mol for alpha cedrene and -8.5 kcal/mol for alpha bisabolol oxide.
- Caspase-1: -7.3 kcal/mol for pinostrobin chalcone and -6.7 kcal/mol for alpha bisabolol oxide.
- COX-2: -6.9 kcal/mol for zingiberene and -7 kcal/mol for pinostrobin chalcone.
- PLA2: -7.5 kcal/mol for both alpha-copaen-11-ol and gamma murolene (**Fig. 2**).

Figure 2. *Molecular docking results illustrated by heatmap [48]*

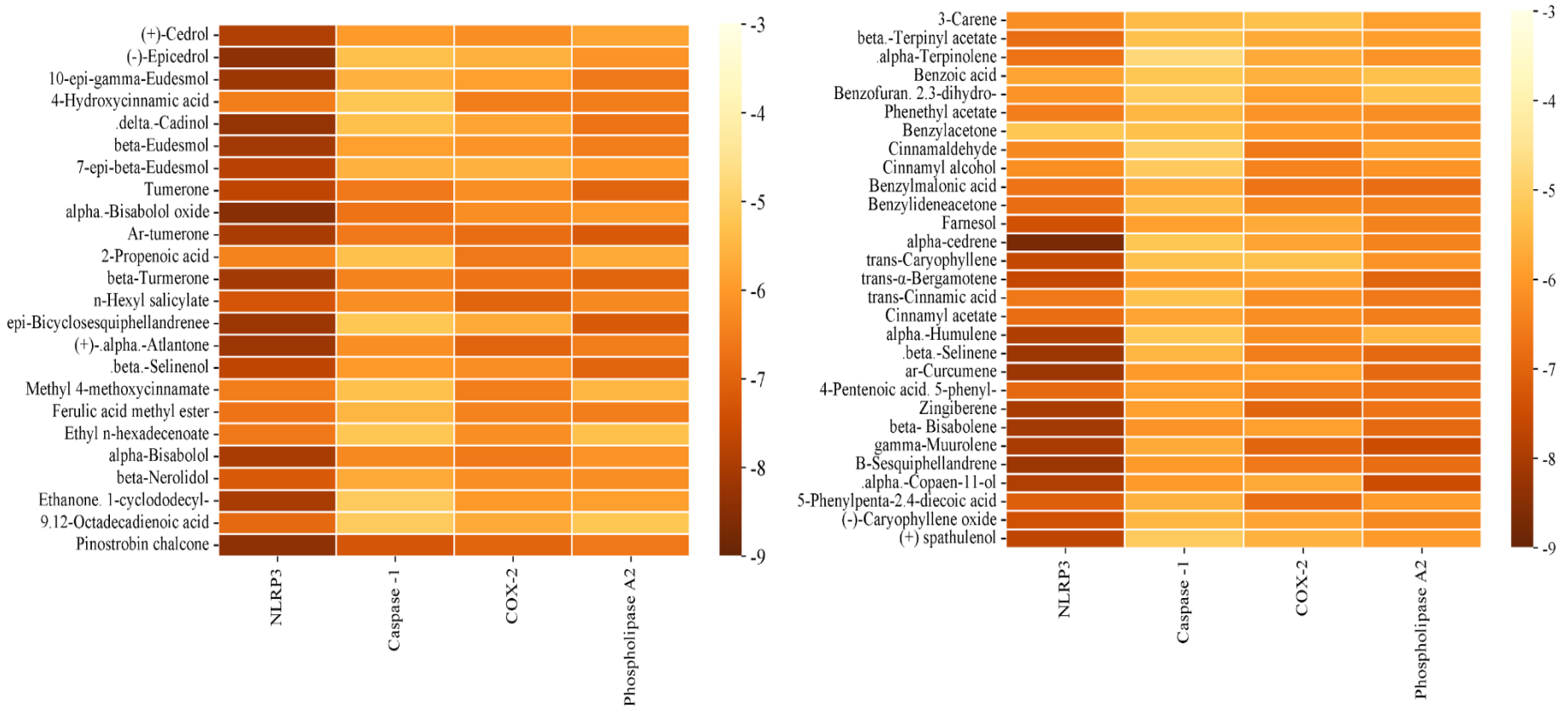

Reference docking was also conducted to validate and calibrate the inhibitory behaviors of the other ligands (**Table 2**). Reference ligands, including a range of known binding affinities, were used to benchmark the performance of diverse docking methods, or scoring functions. Despite PLA2 not having the lowest mean binding affinity, it exhibited the lowest reference binding affinities. In another molecular docking study of PLA2, scores were consistently around -6 kcal/mol for various ligands [49]. PLA2 exhibits an extensive and intricate structure featuring multiple binding sites, highly specific for certain types of phospholipids, potentially leading to inappropriate interactions with ligands. However, the binding affinity value may not consistently serve as the optimal indicator of specific inhibitory interactions, given its susceptibility to various influencing factors. Among these factors, protein flexibility differences play a crucial role, as proteins are dynamic structures capable of undergoing conformational changes that can affect the binding affinity scores of ligands. If the protein undergoes substantial conformational changes during ligand interaction, the docking simulation may fail to capture this behavior, resulting in lower binding affinity predictions.

Table 2. *Binding affinities of reference ligands*

NLRP3		**Caspase-1**		**COX-2**		**Phospholipase A2**	
MCC950	-11,2 kcal/mol	Emricasan	-8 kcal/mol	Flurbiprofen	-8,4 kcal/mol	Varespladib methyl	-5,7 kcal/mol
Oridonin	-9,4 kcal/mol	54675783	-6,2 kcal/mol	Celecoxib	-8,2 kcal/mol	CHEMBL149502	-5,6 kcal/mol

To enhance the accuracy of the predicted binding affinities, inhibition constants were calculated, and the Ki values of the top scores were identified within the range of 0.4-12. This range signifies excellent inhibitory behavior, aligning with the Ki <100 μm rule [50]. Both binding affinities and inhibitory constants highlight the robust binding relations between NLRP3 and ligands. The binding site of NLRP3 exhibits a complex topology characterized by multiple pockets and channels, offering numerous opportunities for ligand interactions, and enhancing binding affinities. Consistent with other molecular docking studies on NLRP3, our findings also reveal elevated binding affinities and conformations [51]. Notably, the highest scores for NLRP3 were -8.7 kcal/mol for alpha cedrene and -8.5 kcal/mol for alpha bisabolol oxide. Upon closer examination (**Fig. 3**), alpha cedrene forms alkyl and pi-alkyl interactions with residues ILE151, TYR168, LEU171, ILE234, PHE373, and PRO412, along with van der Waals interactions with ARG167, THR169, GLY231, TYR381, LEU413, and TRP416 (**Fig. 3a**). Species known for their high alpha-cedrene content, such as *Pinus koraiensis* and *Chamaecyparis obtusa*, exhibit a potent anti-inflammatory profile [52, 53]. Similarly, alpha-bisabolol oxide, as depicted in **Fig. 3b**, engages in alkyl and pi-alkyl interactions with residues TYR168, LEU171, ILE234, PHE373, and PRO412, coupled with van der Waals interactions with ILE151, GLU152, THR169, GLY229, GLY231, THR233, TYR381, and LEU 413 residues. The formation of alkyl interactions between the protein and the ligand augments the binding affinity by causing the hydrophobic regions of the protein to tightly encircle the ligand, forming a more stable complex.

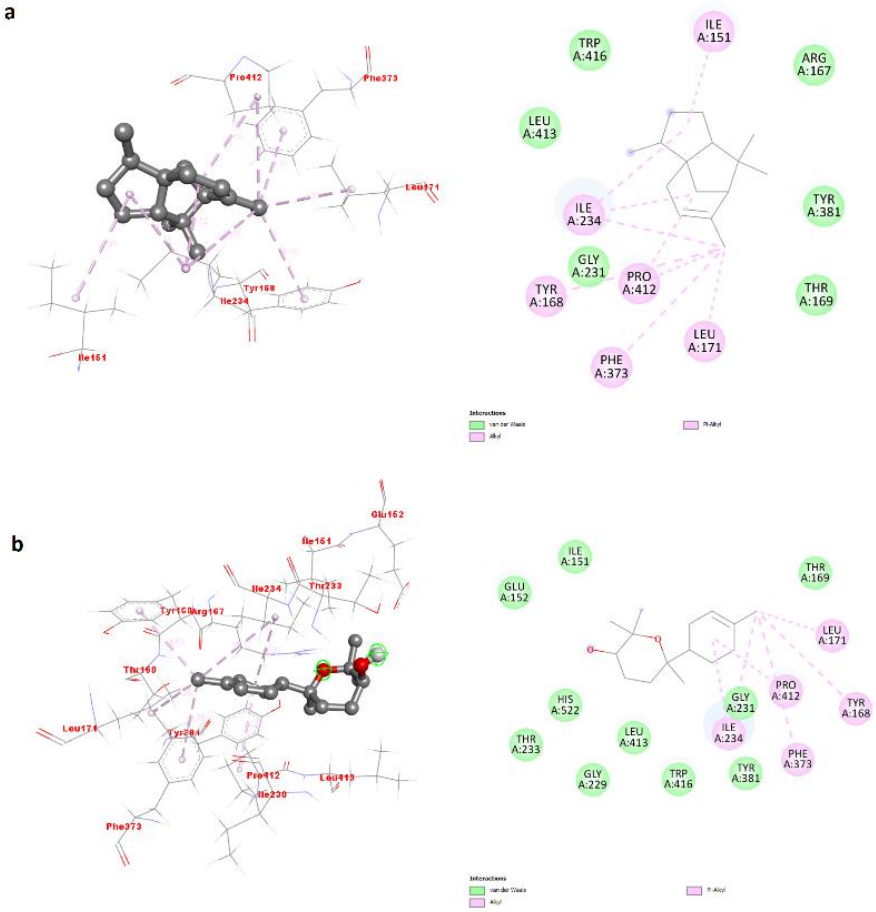

Figure 3. *NLRP3 docking results for top 2 binding affinities (a) alpha cedrene and (b) alpha-bisabolol oxide*

In addition, these interactions contribute to the orientation of the ligand within the protein binding site, increasing the likelihood of other types of interactions [54]. In **Fig. 4a**, pinostrobin chalcone establishes conventional hydrogen bonds with residues LEU258, ARG286, and ARG391, along with alkyl interactions involving ILE243, ILE282, and ALA284. Additionally, it forms amide-pi stacked interactions with GLU241 and GLY242, and van der Waals interactions with residues GLY238, ILE239, ARG240, GLN257, ASN259, and CYS 285. In **Fig. 4b**, alpha bisabolol oxide engages in conventional hydrogen bonds with residues ARG286 and GLU390. It further forms alkyl interactions with ILE243, LEU258, ILE282, and ALA284, as well as van der Waals interactions with residues GLY238, ILE239, ARG240, GLU241, GLY242, CYS285, and PRO335. Notably, the van der Waals interaction involving CYS285 aligns with the electron density specified in a literature study on the 3D structure of caspase 1, which is consistent with our results [55].

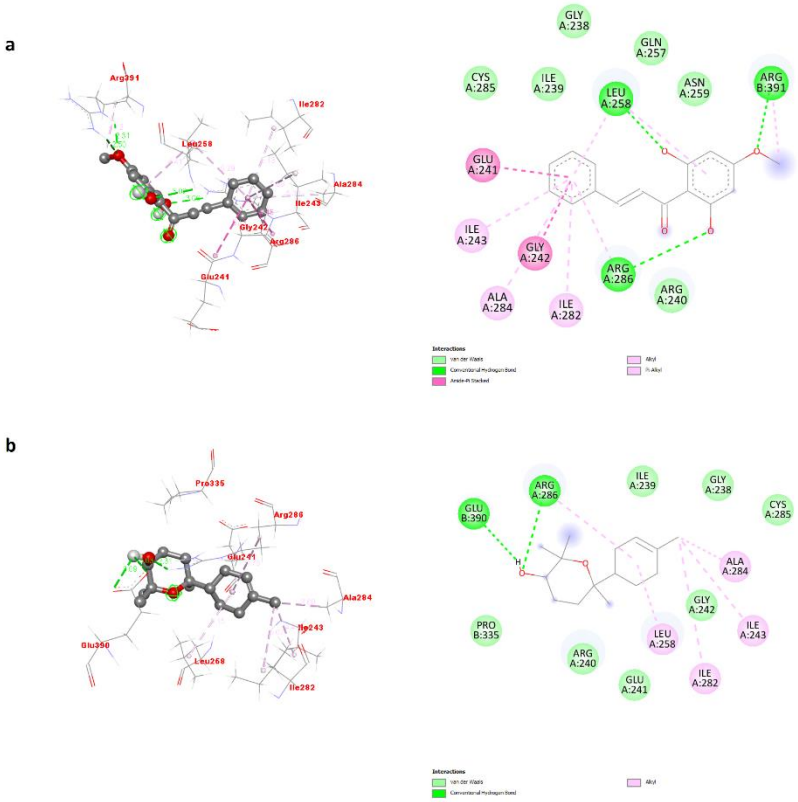

Figure 4. *Caspase-1 docking results for top 2 binding affinities (a) pinostrobin chalcone and (b) alpha-bisabolol oxide*

In **Fig. 5a**, zingiberene establishes a pi-Sigma interaction with the HIS386 residue and alkyl interactions with ALA199, ALA202, HIS207, HIS388, LEU390, and LEU391. Van der Waals interactions are also formed with GLN203, THR206, PHE210, ASN382, TYR385, and TRP 387. Also, in **Fig. 5b**, pinostrobin chalcone forms two conventional hydrogen bonds with THR 212 and HIS386 residues, along with pi-pi T-shaped and carbon-hydrogen bond interactions with HIS388 residue. van der Waals interactions involve ALA202, GLN203, THR206, HIS207, PHE210, LYS211, HIS214, GLN289, VAL291, ASN382, TRP387, HIS388, and VAL447 residues. Zingiberene, a component frequently studied for its anti-inflammatory and anti-apoptotic properties in the literature, is notably associated with ginger species [56]. It has been reported that zingiberene and its derivative biochemical components present in essential oils from species such as *Casearia sylvestris* can effectively suppress inflammatory angiogenesis [57]. Similarly, essential oils derived from *Xylopia laevigata* leaves, rich in gamma-muurolene content, demonstrate pronounced anti-inflammatory and antinociceptive effects [58].

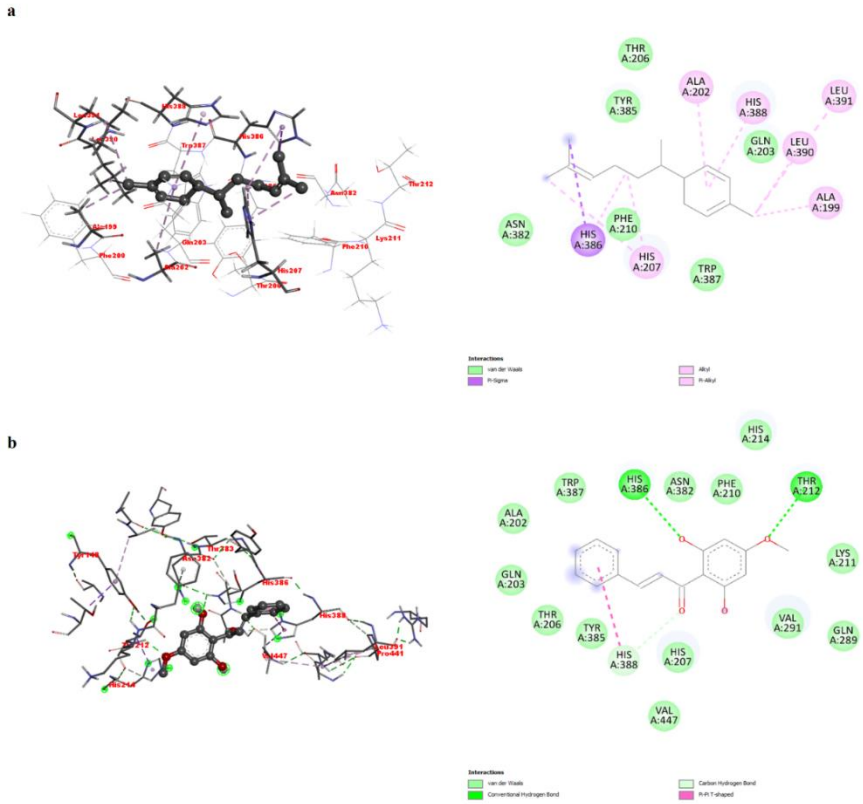

Figure 5. *COX-2 docking results for top 2 binding affinities (a) zingiberene and (b) pinostrobin chalcone*

In **Fig. 6a**, alpha-copaen-11-ol forms a conventional hydrogen bond with GLY30 and alkyl interactions with LEU2, PHE5, LYS6, and ALA23 residues. Additionally, Van der Waals interactions involve residues ILE9, TRP19, PHE22, LYS31, HIS48, ASP49, TYR52, TYR64, and PHE 101. **Fig. 6b** shows that gamma muurolene engages in numerous alkyl interactions with LEU2, PHE5, LYS6, ILE9, TRP19, ALA23, and TYR64 residues, accompanied by van der Waals interactions with similar residues PHE22, CYS29, GLY30, CYS45, HIS48, and PHE101. The observed pi-sigma interactions, occurring between a pi-electron cloud (e.g., aromatic ring) and a sigma bond (e.g., C-H bond), contribute to the overall stability of the ligand-receptor complex by providing additional attractive forces [59]. Additionally, amide-pi stacked interactions, a non-covalent interaction between an amide group and an aromatic ring, further enhance stability by facilitating attractive forces between the ligand and the receptor. Noteworthy is the formation of conventional hydrogen bonds, typically linear and relatively strong interactions between a hydrogen atom and an electronegative atom such as fluorine or nitrogen.

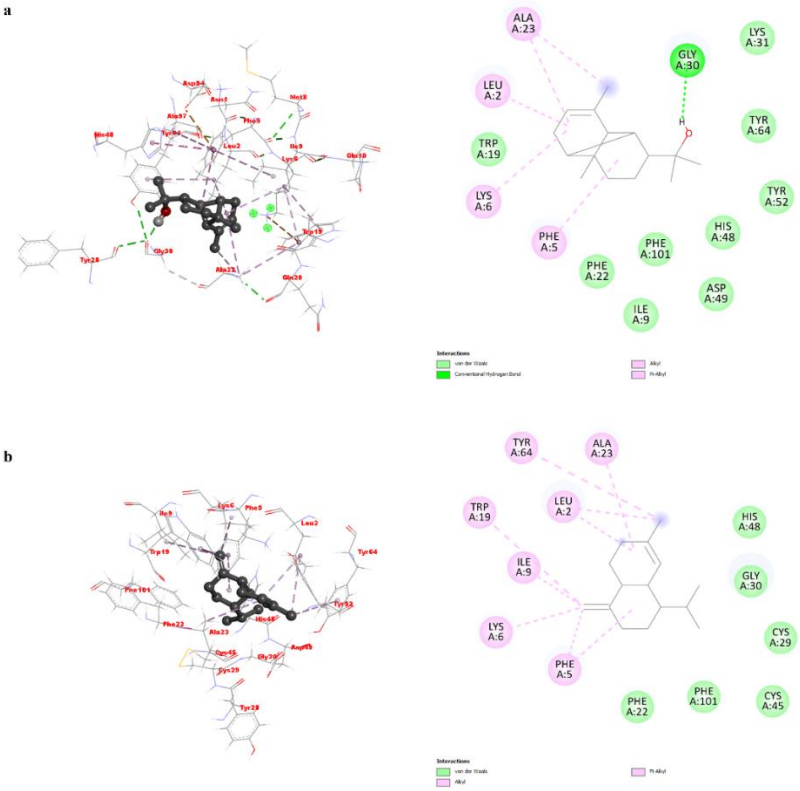

Figure 6. *PLA2 docking results for top 2 binding affinities (a) alpha-copaen-11-ol and (b) gamma murolene*

Remarkably, one of the highest-scoring values across all three inflammation protein targets was observed for alpha bisabolol-derived biochemical compounds. Alpha-bisabolol, a monocyclic sesquiterpene, has been extensively studied for its biotherapeutic effects [60]. Various studies have highlighted the down-regulating effects of alpha-bisabolol and its derivatives on neuroinflammation [61], wound inflammation [62], and gastric inflammation [63], along with a reducing effect on NLRP3 and TNF inflammation biomarkers. Beyond their anti-inflammatory effects, bisabolol derivatives have significant anticancer potential. Studies have reported the reducing effect of alpha-bisabolol on endometrial cancer markers related to COX-2 [64] and its promotion of cell death in glioma cancer cells [65].

Conclusion

In conclusion, the utilizations of *in silico* molecular docking approaches has provided valuable insights into the potential anti-inflammatory effects of propolis volatile compounds. These findings indicate that these compounds hold promise in inhibiting the activity of crucial inflammatory proteins, thereby presenting potential therapeutic benefits for a spectrum of inflammatory diseases. Although further experimental studies are required to validate and corroborate these computational predictions, this research establishes a promising foundation for future investigations exploring the application of propolis as a natural anti-inflammatory agent.

Acknowledgement

This work was supported by Ankara Yıldırım Beyazit University Scientific Research Projects Coordination Unit (BAP/ÖNAP FMG-2021-2254).

References

[1] W. A. Weis *et al.*, "An overview about apitherapy and its clinical applications," *Phytomedicine Plus,* vol. 2, no. 2, p. 100239, 2022/05/01/ 2022.

[2] K. Münstedt and H. Männle, "Apitherapy for menopausal problems," *Arch Gynecol Obstet,* vol. 302, no. 6, pp. 1495-1502, Dec 2020.

[3] B. J. N. Olas, "Bee products as interesting natural agents for the prevention and treatment of common cardiovascular diseases," vol. 14, no. 11, p. 2267, 2022.

[4] F. A. Alassaf, M. H. M. Jasim, M. Alfahad, M. E. Qazzaz, M. N. Abed, and I. A. Thanoon, "Effects of Bee Propolis on FBG, HbA1c, and Insulin Resistance in Healthy Volunteers," (in eng), *Turk J Pharm Sci,* vol. 18, no. 4, pp. 405-409, Sep 1 2021.

[5] E. Nattagh-Eshtivani *et al.*, "Does propolis have any effect on rheumatoid arthritis? A review study," vol. 10, no. 4, pp. 1003-1020, 2022.

[6] A. M. Gómez-Caravaca, M. Gómez-Romero, D. Arráez-Román, A. Segura-Carretero, and A. Fernández-Gutiérrez, "Advances in the analysis of phenolic compounds in products derived from bees," (in eng), *J Pharm Biomed Anal,* vol. 41, no. 4, pp. 1220-34, Jun 16 2006.

[7] V. D. Wagh, "Propolis: a wonder bees product and its pharmacological potentials," (in eng), *Adv Pharmacol Sci,* vol. 2013, p. 308249, 2013.

[8] X. Zheng *et al.*, "Untargeted metabolomics description of propolis's in vitro antibacterial mechanisms against Clostridium perfringens," *Food Chemistry,* vol. 406, p. 135061, 2023/04/16/ 2023.

[9] L. A. Santos *et al.*, "Brazilian Red Propolis shows antifungal and immunomodulatory activities against Paracoccidioides brasiliensis," *Journal of Ethnopharmacology,* vol. 277, p. 114181, 2021/09/15/ 2021.

[10] E. Pelvan *et al.*, "Development of propolis and essential oils containing oral/throat spray formulation against SARS-CoV-2 infection," (in eng), *J Funct Foods,* vol. 97, p. 105225, Oct 2022.

[11] A. Iio *et al.*, "Ethanolic extracts of Brazilian red propolis increase ABCA1 expression and promote cholesterol efflux from THP-1 macrophages," (in eng), *Phytomedicine,* vol. 19, no. 5, pp. 383-8, Mar 15 2012.

[12] L. Alvarenga *et al.*, "To bee or not to bee? The bee extract propolis as a bioactive compound in the burden of lifestyle diseases," (in eng), *Nutrition,* vol. 83, p. 111094, Mar 2021.

[13] V. U. Nna, A. B. Abu Bakar, Z. Zakaria, Z. A. Othman, N. A. C. Jalil, and M. Mohamed, "Malaysian Propolis and Metformin Synergistically Mitigate Kidney Oxidative Stress and Inflammation in Streptozotocin-Induced Diabetic Rats," (in eng), *Molecules,* vol. 26, no. 11, Jun 5 2021.

[14] A. N. Tamfu, O. Ceylan, G. Cârâc, E. Talla, and R. M. Dinica, "Antibiofilm and Anti-Quorum Sensing Potential of Cycloartane-Type Triterpene Acids from Cameroonian Grassland Propolis: Phenolic Profile and Antioxidant Activity of Crude Extract," (in eng), *Molecules,* vol. 27, no. 15, Jul 29 2022.

[15] J.-i. Kashiwakura *et al.*, "Propolis suppresses cytokine production in activated basophils and basophil-mediated skin and intestinal allergic inflammation in mice," *Allergology International,* vol. 70, no. 3, pp. 360-367, 2021/07/01/ 2021.

[16] G. Valenzuela-Barra *et al.*, "Anti-inflammatory activity and phenolic profile of propolis from two locations in Región Metropolitana de Santiago, Chile," *Journal of Ethnopharmacology,* vol. 168, pp. 37-44, 2015/06/20/ 2015.

[17] M. Y. Song, D. Y. Lee, and E. H. Kim, "Anti-inflammatory and anti-oxidative effect of Korean propolis on Helicobacter pylori-induced gastric damage in vitro," (in eng), *J Microbiol,* vol. 58, no. 10, pp. 878-885, Oct 2020.

[18] V. A. Rathinam and K. A. Fitzgerald, "Inflammasome Complexes: Emerging Mechanisms and Effector Functions," (in eng), *Cell,* vol. 165, no. 4, pp. 792-800, May 5 2016.

[19] W.-J. Zhang, S.-J. Chen, S.-C. Zhou, S.-Z. Wu, and H. Wang, "Inflammasomes and Fibrosis," (in English), Review vol. 12, 2021-June-11 2021.

[20] W.-J. Zhang, K.-Y. Li, Y. Lan, H.-Y. Zeng, S.-Q. Chen, and H. Wang, "NLRP3 Inflammasome: A key contributor to the inflammation formation," *Food and Chemical Toxicology,* vol. 174, p. 113683, 2023/04/01/ 2023.

[21] L. Jia *et al.*, "Inhibition of NLRP3 alleviated chemotherapy-induced cognitive impairment in rats," *Neuroscience Letters,* vol. 793, p. 136975, 2023/01/10/ 2023.

[22] A. Ajala, A. Uzairu, G. A. Shallangwa, and S. E. Abechi, "Virtual screening, molecular docking simulation and ADMET prediction of some selected natural products as potential inhibitors of NLRP3 inflammasomes as drug candidates for Alzheimer disease," *Biocatalysis and Agricultural Biotechnology,* vol. 48, p. 102615, 2023/03/01/ 2023.

[23] D. Gao, C.-c. Zheng, J.-p. Hao, C.-c. Yang, and C.-y. Hu, "Icariin ameliorates behavioral deficits and neuropathology in a mouse model of multiple sclerosis," *Brain Research,* vol. 1804, p. 148267, 2023/04/01/ 2023.

[24] D. Jiménez Fernández and M. Lamkanfi, "Inflammatory caspases: key regulators of inflammation and cell death," (in eng), *Biol Chem,* vol. 396, no. 3, pp. 193-203, Mar 2015.

[25] J. Wu *et al.*, "Coptisine from Coptis chinensis blocks NLRP3 inflammasome activation by inhibiting caspase-1," *Pharmacological Research,* vol. 147, p. 104348, 2019/09/01/ 2019.

[26] E. Dore and E. Boilard, "Roles of secreted phospholipase A2 group IIA in inflammation and host defense," *Biochimica et Biophysica Acta (BBA) - Molecular and Cell Biology of Lipids,* vol. 1864, no. 6, pp. 789-802, 2019/06/01/ 2019.

[27] Z. Ju, M. Li, J. Xu, D. C. Howell, Z. Li, and F.-E. Chen, "Recent development on COX-2 inhibitors as promising anti-inflammatory agents: The past 10 years," *Acta Pharmaceutica Sinica B,* vol. 12, no. 6, pp. 2790-2807, 2022/06/01/ 2022.

[28] J. Dai, X. Zhang, L. Li, H. Chen, and Y. Chai, "Autophagy Inhibition Contributes to ROS-Producing NLRP3-Dependent Inflammasome Activation and Cytokine Secretion in High Glucose-Induced Macrophages," *Cellular Physiology and Biochemistry,* vol. 43, no. 1, pp. 247-256, 2017.

[29] A. Manzi *et al.*, "Theoretical evaluation of the malathion and its chemical derivatives interaction with cytosolic phospholipase A2 from zebrafish," *Chemosphere,* vol. 311, p. 136984, 2023/01/01/ 2023.

[30] A. A. Abd El-Wahed *et al.*, "Unravelling the beehive air volatiles profile as analysed via solid-phase microextraction (SPME) and chemometrics," *Journal of King Saud University - Science,* vol. 33, no. 5, p. 101449, 2021/07/01/ 2021.

[31] C. Aslı, N. Vural, and E. J. İ. J. o. P. Şarer, "Determination of volatile compounds in green tea and black tea from Turkey by using HS-SPME and GC-MS," vol. 50, no. 2, pp. 111-115, 2020.

[32] N. Chandra and J. Padiadpu, "Network approaches to drug discovery," (in eng), *Expert Opin Drug Discov,* vol. 8, no. 1, pp. 7-20, Jan 2013.

[33] A. Jakalian, D. B. Jack, and C. I. Bayly, "Fast, efficient generation of high-quality atomic charges. AM1-BCC model: II. Parameterization and validation," (in eng), *J Comput Chem,* vol. 23, no. 16, pp. 1623-41, Dec 2002.

[34] J. Gasteiger and M. Marsili, "A new model for calculating atomic charges in molecules," *Tetrahedron Letters,* vol. 19, no. 34, pp. 3181-3184, 1978/01/01/ 1978.

[35] O. Trott and A. J. Olson, "AutoDock Vina: improving the speed and accuracy of docking with a new scoring function, efficient optimization, and multithreading," (in eng), *J Comput Chem,* vol. 31, no. 2, pp. 455-61, Jan 30 2010.

[36] R. G. Coleman, M. Carchia, T. Sterling, J. J. Irwin, and B. K. Shoichet, "Ligand pose and orientational sampling in molecular docking," (in eng), *PLoS One,* vol. 8, no. 10, p. e75992, 2013.

[37] J. Eberhardt, D. Santos-Martins, A. F. Tillack, and S. Forli, "AutoDock Vina 1.2.0: New Docking Methods, Expanded Force Field, and Python Bindings," *Journal of Chemical Information and Modeling,* vol. 61, no. 8, pp. 3891-3898, 2021/08/23 2021.

[38] J. Jiao, G. Zhao, Y. Wang, P. Ren, and M. Wu, "MCC950, a Selective Inhibitor of NLRP3 Inflammasome, Reduces the Inflammatory Response and Improves Neurological Outcomes in Mice Model of Spinal Cord Injury," (in eng), *Front Mol Biosci,* vol. 7, p. 37, 2020.

[39] H. He *et al.*, "Oridonin is a covalent NLRP3 inhibitor with strong anti-inflammasome activity," (in eng), *Nat Commun,* vol. 9, no. 1, p. 2550, Jun 29 2018.

[40] F. J. Barreyro *et al.*, "The pan-caspase inhibitor Emricasan (IDN-6556) decreases liver injury and fibrosis in a murine model of non-alcoholic steatohepatitis," (in eng), *Liver Int,* vol. 35, no. 3, pp. 953-66, Mar 2015.

[41] M. Chen *et al.*, "Minocycline inhibits caspase-1 and caspase-3 expression and delays mortality in a transgenic mouse model of Huntington disease," (in eng), *Nat Med,* vol. 6, no. 7, pp. 797-801, Jul 2000.

[42] R. Agrawal, C. S. Lee, J. J. Gonzalez-Lopez, S. Khan, V. Rodrigues, and C. Pavesio, "Flurbiprofen: A Nonselective Cyclooxygenase (COX) Inhibitor for Treatment of Noninfectious, Non-necrotizing Anterior Scleritis," (in eng), *Ocul Immunol Inflamm,* vol. 24, no. 1, pp. 35-42, 2016.

[43] J. L. Mateos, "[Selective inhibitors of cyclooxygenase-2 (COX-2), celecoxib and parecoxib: a systematic review]," (in spa), *Drugs Today (Barc),* vol. 46 Suppl A, pp. 1-

25, Feb 2010. Inhibidores selectivos de la ciclooxigenasa-2 (COX-2), celecoxib y parecoxib: una revisión sistemática.

[44] M. Karakas and W. Koenig, "Varespladib methyl, an oral phospholipase A2 inhibitor for the potential treatment of coronary artery disease," (in eng), *IDrugs,* vol. 12, no. 9, pp. 585-92, Sep 2009.

[45] J. Lättig *et al.*, "Mechanism of inhibition of human secretory phospholipase A2 by flavonoids: rationale for lead design," (in eng), *J Comput Aided Mol Des,* vol. 21, no. 8, pp. 473-83, Aug 2007.

[46] V. Bankova *et al.*, "Standard methods for Apis mellifera propolis research," *Journal of Apicultural Research,* vol. 58, no. 2, pp. 1-49, 2019/03/15 2019.

[47] Z. Wang *et al.*, "NLRP3 Inflammasome and Inflammatory Diseases," (in eng), *Oxid Med Cell Longev,* vol. 2020, p. 4063562, 2020.

[48] D. Tang *et al.*, "SRplot: A free online platform for data visualization and graphing," *PLOS ONE,* vol. 18, no. 11, p. e0294236, 2023.

[49] J. Bakht, A. Islam, H. Ali, M. Tayyab, and M. J. A. J. o. B. Shafi, "Antimicrobial potentials of Eclipta alba by disc diffusion method," vol. 10, no. 39, pp. 7658-7667, 2011.

[50] X. Zheng and J. Polli, "Identification of inhibitor concentrations to efficiently screen and measure inhibition Ki values against solute carrier transporters," (in eng), *Eur J Pharm Sci,* vol. 41, no. 1, pp. 43-52, Sep 11 2010.

[51] D. F. Sayed, A. H. Afifi, A. Temraz, and A. H. Ahmed, "Metabolic Profiling of Mimusops elengi Linn. Leaves extract and in silico anti-inflammatory assessment targeting NLRP3 inflammasome," *Arabian Journal of Chemistry,* vol. 16, no. 6, p. 104753, 2023/06/01/ 2023.

[52] T. C. Chien, S. F. Lo, and C. L. Ho, "Chemical composition and anti-inflammatory activity of Chamaecyparis obtusa f.formosana wood essential oil from Taiwan," (in eng), *Nat Prod Commun,* vol. 9, no. 5, pp. 723-6, May 2014.

[53] C. Ahn, J. W. Kim, M. J. Park, S. R. Kim, S. S. Lee, and E. B. Jeung, *Anti-inflammatory effects of natural volatile organic compounds from Pinus koraiensis and Larix kaempferi in mouse model*. J Biomed Res. 2019 Sep;33(5):343-50. doi: 10.7555/JBR.32.20180058.

[54] C. W. Fong, "Predicting hydrophobic alkyl-alkyl and perfluoroalkyl-perfluoroalkyl van der Waals dispersion interactions and their potential involvement in protein folding and the binding of drugs in hydrophobic pockets," 2019.

[55] T. O'Brien *et al.*, "Structural analysis of caspase-1 inhibitors derived from Tethering," (in eng), *Acta Crystallogr Sect F Struct Biol Cryst Commun,* vol. 61, no. Pt 5, pp. 451-8, May 1 2005.

[56] J. Li, R. Thangaiyan, K. Govindasamy, and J. Wei, "Anti-inflammatory and anti-apoptotic effect of zingiberene on isoproterenol-induced myocardial infarction in experimental animals," (in eng), *Hum Exp Toxicol,* vol. 40, no. 6, pp. 915-927, Jun 2021.

[57] B. A. Ferreira *et al.*, "α-zingiberene, a sesquiterpene from essential oil from leaves of Casearia sylvestris, suppresses inflammatory angiogenesis and stimulates collagen deposition in subcutaneous implants in mice," (in eng), *Nat Prod Res,* vol. 36, no. 22, pp. 5858-5862, Nov 2022.

[58] J. C. Queiroz *et al.*, "Evaluation of the anti-inflammatory and antinociceptive effects of the essential oil from leaves of Xylopia laevigata in experimental models," (in eng), *ScientificWorldJournal,* vol. 2014, p. 816450, 2014.

[59] M. W. Krone, C. R. Travis, G. Y. Lee, H. J. Eckvahl, K. N. Houk, and M. L. Waters, "More Than π–π–π Stacking: Contribution of Amide−π and CH−π Interactions to Crotonyllysine Binding by the AF9 YEATS Domain," *Journal of the American Chemical Society,* vol. 142, no. 40, pp. 17048-17056, 2020/10/07 2020.

[60] L. B. Eddin *et al.*, "Health Benefits, Pharmacological Effects, Molecular Mechanisms, and Therapeutic Potential of α-Bisabolol," (in eng), *Nutrients,* vol. 14, no. 7, Mar 25 2022.

[61] H. Javed *et al.*, "α-Bisabolol, a Dietary Bioactive Phytochemical Attenuates Dopaminergic Neurodegeneration through Modulation of Oxidative Stress, Neuroinflammation and Apoptosis in Rotenone-Induced Rat Model of Parkinson's disease," (in eng), *Biomolecules,* vol. 10, no. 10, Oct 8 2020.

[62] L. G. Solovăstru, A. Stîncanu, A. De Ascentii, G. Capparé, P. Mattana, and D. Vâţă, "Randomized, controlled study of innovative spray formulation containing ozonated oil and α-bisabolol in the topical treatment of chronic venous leg ulcers," (in eng), *Adv Skin Wound Care,* vol. 28, no. 9, pp. 406-9, Sep 2015.

[63] M. I. Ortiz, R. Cariño-Cortés, H. A. Ponce-Monter, G. Castañeda-Hernández, and A. E. Chávez-Piña, "Pharmacological interaction of α-bisabolol and diclofenac on nociception, inflammation, and gastric integrity in rats," (in eng), *Drug Dev Res,* vol. 79, no. 1, pp. 29-37, Feb 2018.

[64] D. Fang, H. Wang, M. Li, and W. Wei, "α-bisabolol enhances radiotherapy-induced apoptosis in endometrial cancer cells by reducing the effect of XIAP on inhibiting caspase-3," (in eng), *Biosci Rep,* vol. 39, no. 6, Jun 28 2019.

[65] F. B. Mendes *et al.*, "Alpha-bisabolol Promotes Glioma Cell Death by Modulating the Adenosinergic System," (in eng), *Anticancer Res,* vol. 37, no. 4, pp. 1819-1823, Apr 2017.